




# Diagnostic performance of node-RADS classification for primary lymph node assessment in rectal cancer: a modality benchmarking study

Li Jiang<sup>1,3</sup> · Zijian Zhuang<sup>1</sup> · Xi Tang<sup>3</sup> · Fugang Zhang<sup>3</sup> · Haitao Zhu<sup>2</sup> · Xuewen Xu<sup>1</sup> · Dongqing Wang<sup>1,2</sup> · Lirong Zhang<sup>1,2</sup> 

Received: 4 March 2025 / Accepted: 3 April 2025 / Published online: 19 April 2025  
© The Author(s) 2025

## Abstract

**Purpose** To evaluate how well the Node Reporting and Data System (Node-RADS) diagnoses lymph node involvement (LNI) in the initial stages of rectal cancer, utilizing contrast-enhanced CT (CE-CT), T2-weighted MRI (T2WI) and contrast-enhanced T1-weighted MRI (T1CE).

**Methods** This retrospective study included 113 rectal cancer patients who underwent radical surgery without neoadjuvant therapy. Two radiologists independently assessed regional lymph nodes using the highest Node-RADS classification and histopathology as reference criteria. Diagnostic performance was evaluated using receiver operating characteristic (ROC) curve analysis. Statistical analysis was performed using the McNemar test with Bonferroni correction for multiple comparisons.

**Results** Node-RADS showed improved diagnostic performance over short-axis diameter (SAD) in all modalities (AUC: 0.838 vs. 0.744 for CE-CT, 0.845 vs. 0.747 for T2WI, 0.853 vs. 0.786 for T1CE; all  $P < 0.05$ ). The sensitivity and specificity of Node-RADS across three modalities ranged from 76.19–78.57% and 91.55–92.96%, respectively. Pairwise comparisons of sensitivity and specificity among the three modalities showed no significant differences after Bonferroni correction (all McNemar test  $P = 1.0$ ). There was no significant difference in Node-RADS performance among the three modalities (all  $P > 0.05$ ). The weighted kappa values were 0.742–0.798.

**Conclusion** Node-RADS demonstrated superior diagnostic performance over SAD measurements and similar diagnostic effectiveness in assessing LNI for primary rectal cancer stages across CE-CT, T2WI, and T1CE.

**Keywords** Rectal cancer · Lymph node · Computed tomography · Magnetic resonance imaging · Node reporting and data system

## Introduction

Globally, colorectal cancer ranks among the most prevalent cancer forms, with rectal cancer representing about a third of all colorectal cancer instances (Bray et al. 2024; Siegel et al. 2023). Lymph node involvement (LNI) represents the most common mode of metastasis in rectal cancer and has a critical role in determining patient management strategies and predicting postoperative outcomes (Dekker et al. 2019; Akkaya et al. 2024; Kapiteijn et al. 2001). The European Society of Gastrointestinal and Abdominal Radiology (ESGAR) consensus has sought to address this issue by integrating size and morphological criteria; however, its applicability is constrained by its disease-specific and

Li Jiang and Zijian Zhuang contribute equally to this work.

✉ Dongqing Wang  
wangdongqing71@163.com

✉ Lirong Zhang  
tianchen861@ujs.edu.cn

<sup>1</sup> Department of Medical Imaging, The Affiliated Hospital of Jiangsu University, Zhenjiang, Jiangsu Province 212001, China

<sup>2</sup> Institute of Radiology and Artificial Intelligence, Jiangsu University, Zhenjiang, Jiangsu Province 212001, China

<sup>3</sup> School of Medicine, Jiangsu University, Zhenjiang, Jiangsu Province 212001, China

MRI-specific approach (Beets-Tan et al. 2018). A recent multicenter audit in the United Kingdom highlighted significant variability in lymph node assessment methodologies, with radiologists employing diverse combinations of criteria, including ESGAR guidelines, chemical shift imaging, nodal signal intensity, and morphological features (Robinson et al. 2024). While the condition of lymph nodes is vital for categorizing risks, in contrast to other prevalent reporting mechanisms like PI-RADS for prostate and TI-RADS for thyroid scans, uniform systems for reporting lymph node assessments remain underdeveloped (Turkbey et al. 2019; Tessler et al. 2017).

In 2021, Elsholtz et al. introduced the Node Reporting and Data System v1.0 (Node-RADS v1.0) (Elsholtz et al. 2021), which relies on a five-point Likert scale-based scoring system (from 1 “very low likelihood” to 5 “very high likelihood”) to standardize the imaging evaluation of tumor lymph nodes (LN). This system integrates key morphological features of LNs, including size, texture, border characteristics, and shape, into a comprehensive three-level flowchart. It offers standardized terminology and a structured reporting framework, facilitating consistent and reproducible lymph node assessment. The Node-RADS version 1.0 is applicable to both computed tomography (CT) and magnetic resonance imaging (MRI), irrespective of anatomical location or cancer type. The clinical utility of Node-RADS has been extensively validated across various malignancies, including lung (Meyer et al. 2022), breast (Pediconi et al. 2024), gastric (Loch et al. 2024), and cervical (Wu et al. 2024) cancers. Furthermore, its efficacy as a robust tool for lymph node assessment has been substantiated in a recent meta-analysis conducted by Zhong et al. (Zhong et al. 2024). In the context of rectal cancer, Niu et al. validated the diagnostic performance of Node-RADS independently for both CT and MRI, demonstrating its superiority over the ESGAR classification system (AUC 0.862 vs. 0.797,  $P=0.040$ ) (Niu et al. 2024, 2025). While Node-RADS has been evaluated in 10 CT and 7 MRI studies, no direct head-to-head comparison of CT and MRI has been conducted for the same patients and lymph nodes in these investigations. Consequently, the influence of cancer type and imaging modality on the diagnostic performance of Node-RADS remains uncertain, warranting further investigation.

MRI is universally recommended as the standard imaging modality for rectal cancer staging (Fernandes et al. 2022). T2-weighted imaging (T2WI) is highly effective in delineating lymph node morphology and internal architecture, owing to its exceptional soft tissue contrast resolution. Contrast-enhanced T1-weighted imaging (T1CE) can provide valuable information about nodal texture and enhancement patterns. In clinical practice, various constraints such as contraindications, claustrophobia, or limited MRI access

often necessitate the use of CT as an alternative imaging modality. While Node-RADS was developed to be applicable to both CT and MRI, comparative evaluation of its performance across different imaging modalities remains limited. Therefore, we designed this study to evaluate Node-RADS performance across CE-CT, T2WI, and T1CE. This systematic comparison would validate the reliability of Node-RADS criteria across different imaging modalities.

## Materials and methods

### Patients

Approval was obtained from the ethics committee of the Affiliated Hospital of Jiangsu University. The procedures used in this study adhere to the tenets of the Declaration of Helsinki.

We retrospectively analyzed consecutive patients with rectal cancer treated at our institution between June 2017 and December 2023. A total of 179 patients who had both pretreatment contrast-enhanced abdominal CT and pelvic MRI scans were included. Inclusion criteria were: (1) those who underwent total mesorectal excision (TME); (2) rectal adenocarcinoma was confirmed by postoperative pathology. To avoid potential confounding effects of treatment-induced changes in tumor characteristics, patients with a history of neoadjuvant therapy were excluded. Other exclusion criteria included history or concurrent malignancy, poor image quality, a time interval between CT/MRI examination and surgery > 2 weeks. Inclusion and exclusion criteria are shown in Figure S1.

Our institutional imaging strategy for rectal cancer staging follows multidisciplinary treatment guidelines and NCCN recommendations, utilizing MRI for local staging and non-contrast chest CT combined with contrast-enhanced abdominal CT for distant metastasis evaluation (Benson et al. 2022). For each patient, we retrospectively collected the following clinical and pathological data from our Electronic Medical Record system and Picture Archiving and Communication Systems: age, gender, preoperative serum carcinoembryonic antigen (CEA), preoperative serum carbohydrate antigen 19–9 (CA 19–9), type of surgery (abdominoperineal excision or low anterior resection), tumor location (proximal, mid, distal), pathological grade, status of perineural invasion, number of lymph nodes removed during surgery, and images from both CT and MRI.

### CT and MRI assessment

CT and MRI protocols are explained in the supplementary materials.

## Node-RADS assessment

Both experienced radiologists have more than four years of experience in abdominal imaging diagnosis and have trained in the unified Node-RADS assessment to assess LN status (reader 1 and reader 2). Image analysis was performed independently by two radiologists for all 113 patients. The radiologists were only aware of the diagnosis of rectal cancer without access to clinical staging, pathological outcomes, or other examination results. All images were reviewed on dedicated workstations with standardized display settings and adjustable window width and level parameters. A minimum 4-week interval was maintained between the evaluations of different imaging modalities to minimize recall bias. For each modality, the evaluation was completed within two weeks. Discrepancies were resolved by inviting a third, more experienced radiologist (reader 3, with over 20 years of experience in abdominal imaging diagnosis), and the selection made by this expert was used for further analysis. For interobserver agreement analysis, measurements from reader 1 and reader 2 were used. Three sets of data were independently collected.

Suspicious regional lymph nodes (including mesorectal, superior rectal, inferior mesenteric, internal iliac, obturator, and inferior rectal nodes, as defined by the AJCC TNM 8th edition (Weiser 2018) were identified on the portal venous phase of CE-CT, optimal planes in non-fat-suppressed T2WI (coronal, sagittal, or axial), and delayed phase of axial T1CE images.

The Node-RADS scoring system (version 1.0) utilizes a five-point scale (1–5) to indicate the probability of lymph node metastasis, where scores of 1, 2, 3, 4, and 5 represent very low, low, intermediate, high, and very high likelihood, respectively (Elsholtz et al. 2021). In the TNM staging framework, Node-RADS 1 and 2 are suggested to be reported as N(–), whereas Node-RADS 4 and 5 are recommended to be classified as N(+). The reporting of Node-RADS 3 should be guided by the primary stage and histological grade of the primary tumor. The scoring system integrates two primary assessment components: size evaluation and morphological features. Size assessment categorizes lymph nodes into three groups: normal-sized, enlarged, or bulk, with size thresholds varying according to anatomical location. Morphological assessment considers three key characteristics: internal texture, border characteristics, and nodal shape. For texture evaluation, nodes are classified as homogeneous (0 points), heterogeneous (1 point), partially necrotic (2 points), or extensively necrotic (3 points). Border features are categorized as well-defined (0 points) or irregular/poorly defined (1 point). Shape assessment includes preserved fatty hilum or kidney-bean appearance (0 points) and round configuration without fatty hilum (1 point).

In the assessment of rectal cancer lymph nodes, the Node-RADS scoring process consists of two sequential steps. First, lymph nodes are categorized by size into normal (short-axis diameter [SAD] < 5 mm), enlarged (SAD ≥ 5 mm), or bulk (any axis ≥ 30 mm). Second, configuration features, including texture, border, and shape are evaluated and scored. The final Node-RADS category is then determined by combining the size classification with the sum of configuration scores. The categories, corresponding definitions, and characteristics of the specific criteria are illustrated in *Figure S2*.

The LN with the highest score should be reported for each patient, as recommended by Node-RADS. In our study, the highest-scoring node was evaluated for each imaging modality per patient. Characteristics such as short SAD, texture, border, and shape of the highest classified lymph node in each modality were recorded. When multiple lymph nodes showed the same maximum score, a target node was selected to record characteristics according to the following criteria: (1) LN with a larger SAD (difference in SAD ≥ 1 mm); (2) LN with heterogeneous texture (necrosis or mucinous texture); (3) spherical rather than elliptical lymph nodes; and (4) lymph nodes located above rather than below the tumor. Based on the Node-RADS (version 1.0) scoring system, scores ranging from 1 to 5 were assigned to determine the likelihood of locoregional LNI (*Figure S2*). For each patient, we defined the highest Node-RADS score among the three modalities as Node-RADS<sub>max</sub> and the lowest Node-RADS score among the three modalities as Node-RADS<sub>min</sub>. The SAD of LNs was determined by the mean measurements of the two observers. Examples of the same lymph node being classified differently in different modalities are depicted in Fig. 1.

## Surgery and pathological assessment

All patients underwent oncologic abdominoperineal excision or low anterior resection with regional lymphadenectomy. Extended lymphadenectomy, including lateral node dissection, was performed only in patients with radiologically suspicious lateral nodal involvement following multidisciplinary assessment, considering that these nodes lie outside the mesorectal fascia and the potential risks of surgical complications. All surgical specimens were obtained within two weeks after the last imaging examination.

The surgical specimens were fixed in 10% neutral buffered formalin for 24–48 h. All lymph nodes identified in the surgical specimens were harvested for pathological analysis. The harvested lymph nodes were serially sectioned at 3-mm intervals, embedded in paraffin, and stained with hematoxylin and eosin. Two pathologists independently evaluated all specimens and were blinded to the imaging results during their assessment. Lymph node involvement

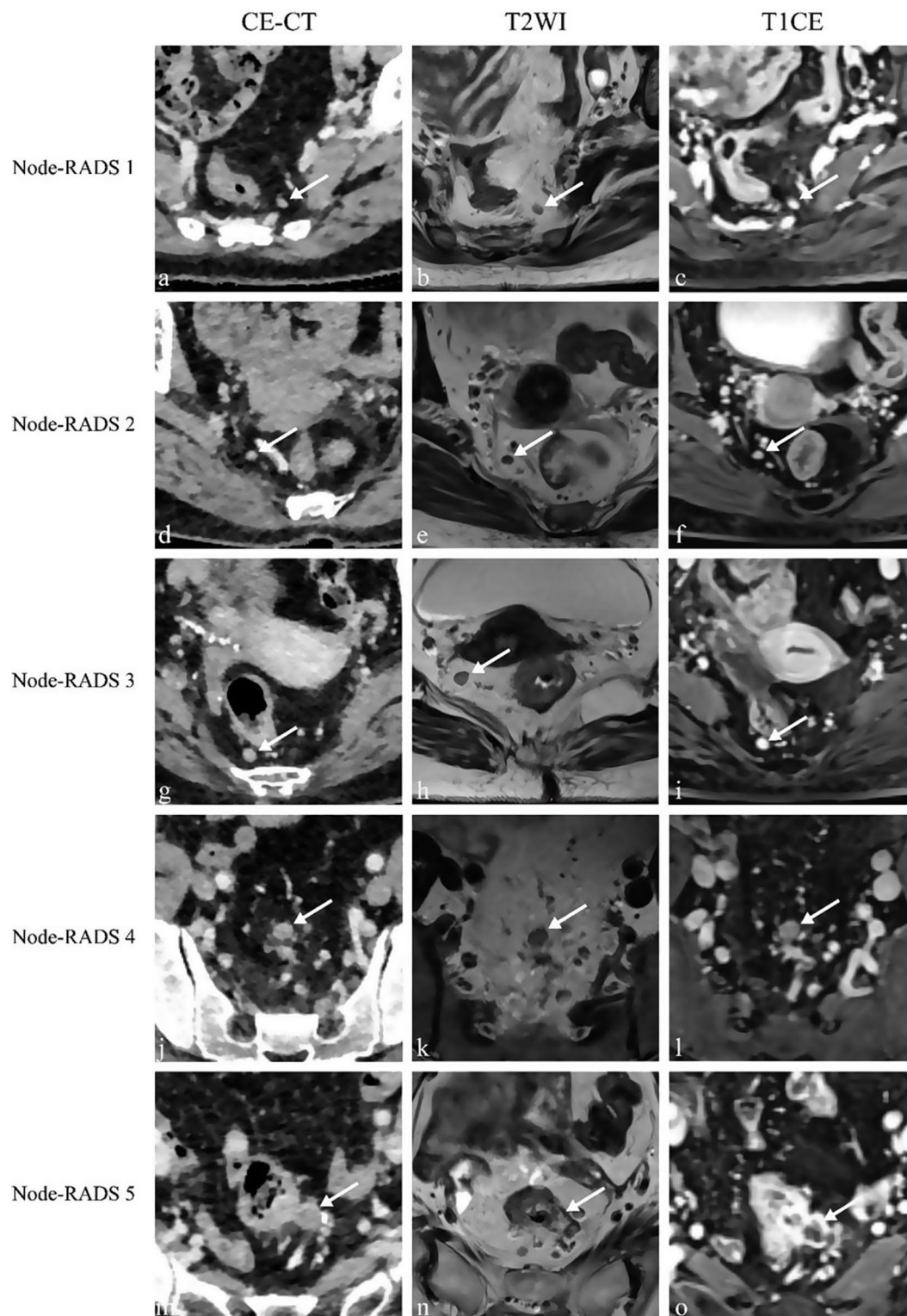


**Fig. 1** Representative lymph nodes (arrow) with the highest Node-RADS score in each category. Each row represents a single patient, with the same Node-RADS score assigned across all three modalities. The white boxes indicate the region of interest containing the representative lymph nodes. (a–c) Node-RADS 1 case: SAD < 5 mm, oval without fatty hilum (0 points), smooth borders (0 points), homogeneous (0 points) in three modalities. (d–f) Node-RADS 2 case: SAD < 5 mm, spherical without fatty hilum (1 point), smooth borders (0 points), homogeneous (0 points) in three modalities. (g–i) Node-

RADS 3 case: SAD > 5 mm, spherical without fatty hilum (1 point), smooth borders (0 points), homogeneous (0 points) in three modalities. (j–l) Node-RADS 4 case: SAD > 5 mm, spherical without fatty hilum (1 point), smooth borders (0 points), heterogeneous (1 point) in three modalities. (m–o) Node-RADS 5: three modalities demonstrate similar features except for the texture subcategory. SAD > 5 mm, spherical without fatty hilum (1 point), irregular borders (1 point), focal necrosis on CE-CT (2 points), mucinous texture on T2WI (3 points) and gross necrosis on T1CE (3 points)



was determined based on established criteria: the presence of tumor cells within the lymph node capsule or subcapsular sinus. The presence of tumor deposits without residual lymph node structure was also recorded. In case of discrepancy, consensus was reached through discussion.

Pathological TNM staging was conducted on formalin-fixed surgical specimens following AJCC 8th edition guidelines (Weiser 2018). Node status was based on the presence (pN+) or absence (pN-) of lymph node metastasis.

## Statistical analysis

Quantitative variables were presented as medians with interquartile ranges (IQRs). Categorical variables were expressed as frequencies and percentages. Comparisons between groups were analyzed using Mann–Whitney U tests for continuous variables and Pearson's Chi-squared test (or Fisher exact test for small data sets) for categorical variables. The inter-reader agreement between reader 1 and reader 2 was evaluated utilizing Cohen's weighted kappa. The intraclass correlation coefficient (ICC) was calculated to measure the consistency of SAD. Receiver operating characteristic (ROC) curves were used to assess the diagnostic performance. We also investigated the diagnostic performance of different SAD cut-off values, ranging from 3 mm to 10 mm. The calculation of the Youden index (YI), and sensitivity, specificity, positive likelihood ratio (LR+), negative likelihood ratio (LR-), diagnostic odds ratio (DOR), positive predictive value (PPV), negative predictive value (NPV), accuracy (ACC), and area under the curve (AUC), was performed. The McNemar test was used to compare the sensitivity, specificity, and accuracy of different Node-RADS grouping methods, while the DeLong test was used to compare the AUCs. For multiple comparisons, P values were adjusted using the Bonferroni correction method. An integrated discrimination improvement (IDI) test was performed to evaluate the incremental diagnostic value among different methods. Statistical analyses were performed using IBM SPSS Statistics Software (version 26.0; IBM Corp.), MedCalc (version 15.2.2, MedCalc Software bvba), and R software (version 4.0.3). All hypothesis tests were two-tailed; *P*-values < 0.05 represented statistically significant differences.

## Results

### The clinical information of patients

A total of 179 consecutive patients with rectal cancer were initially enrolled in this study. 66 (36.9%) were excluded for the following reasons: 28 patients (15.6%) had received

preoperative neoadjuvant chemoradiotherapy, 15 patients (8.4%) had concurrent malignancies or a history of malignancy, 20 patients (11.2%) had insufficient MRI or CT image quality for assessment, and for 3 patients (1.7%), the time interval between MRI/CT examination and surgery exceeded 2 weeks. The remaining 113 patients were included in the final analysis (mean age: 66 years, range 59–73 years, 73 men). Pathological examination identified 42 (37.2%) patients as pN+. Preoperative serum CEA levels were significantly higher in the pN+ group than in the pN- group (*P*=0.045). Furthermore, differences in pathological tumor stage, histological grading, perineural invasion, and lymphovascular invasion were observed between the two groups (*P*=0.001–0.045). No statistically significant differences were observed between the two groups with respect to age, gender, CA19-9, or the number of lymph nodes removed during surgery between the two groups (*P*=0.070–0.840). A comprehensive overview of the clinical and histological characteristics is provided in Table 1.

### Interobserver agreement assessment

The interobserver agreement for Node-RADS scores was substantial on CE-CT, T2WI, and T1CE (weighted kappa value 0.742, 0.776, and 0.798, respectively). The ICC for assessing SAD on CE-CT, T2WI, and T1CE were 0.974, 0.979, and 0.980, respectively. For the evaluation of shape, border, and texture, the weighted kappa values were 0.666, 0.774, and 0.694 for CE-CT; 0.864, 0.758, and 0.667 for T2WI, and 0.721, 0.613, and 0.851, for T1CE, respectively (Table S1). Discrepancies between reader 1 and reader 2 occurred in 40 cases (35.4%) for CE-CT, 36 cases (31.9%) for T2WI, and 34 cases (30.1%) for T1CE, which were subsequently reviewed and adjudicated by reader 3.

### Analyses of size criterion

A total of 72.57% (82/113) of the highest-scoring nodes were identified on CE-CT, 65.49% (74/113) on T2WI, and 61.95% (70/113) on T1CE had a SAD of > 5 mm. The results present the diagnostic performance of each cut-off value of the SADs (Table S2). The SAD with the highest Youden index was 7 mm for CE-CT (accuracy: 71.68%, sensitivity: 59.52%, specificity: 77.46%), 6 mm for T2WI (accuracy: 69.91%, sensitivity: 71.43%, specificity: 69.01%), and 6 mm for T1CE (accuracy: 74.34%, sensitivity: 73.81%, specificity: 74.65%). The accuracy of 5 mm, 10 mm, and the optimal cutoff values were 57.52%, 70.80%, 73.45% for CE-CT; 61.06%, 69.91%, 71.68% for T2WI, and 66.37%, 69.91%, 74.34% for T1CE, respectively.

**Table 1** Clinical and pathologic characteristics of study patients

Parameters	ALL n = 113	pN- n = 71	pN+ n = 42	<i>p</i> -value
Age, years	66 [59; 73]	67 [57; 73]	66 [61; 72]	0.530
Gender, n (%)				0.720
Male	73 (64.6%)	45 (63.4%)	28 (66.7%)	
Female	40 (35.4%)	26 (36.6%)	14 (33.3%)	
CEA, (ng/ml)	3.9 [2.2; 7.1]	3.3 [1.8; 6.4]	5.2 [3.3; 8.6]	0.045
CA19-9, (U/ml)	7.2 [4.0; 13.5]	6.6 [3.5; 10.5]	10.0 [4.6; 18.8]	0.070
Type of surgery				0.840
APE	39 (34.5%)	25 (35.2%)	14 (33.3%)	
LAR	74 (65.5%)	46 (64.8%)	28 (66.7%)	
Location				0.570
Proximal	22 (19.5%)	15 (21.1%)	7 (16.7%)	
Mid	60 (53.1%)	35 (49.3%)	25 (59.5%)	
Distal	31 (27.4%)	21 (29.6%)	10 (23.8%)	
Pathological Tumor stage, n (%)				0.002
pT1-2	39 (34.5%)	33 (46.5%)	6 (14.3%)	
pT3-4	74 (65.5%)	38 (53.5%)	36 (85.7%)	
Histology Grading, n (%)				0.045
Grade I/II	87 (77.0%)	59 (83.1%)	28 (66.7%)	
Grade III/IV	26 (23.0%)	12 (16.9%)	14 (33.3%)	
Perineural Invasion, n (%)				0.008
Absence	38 (33.6%)	26 (36.6%)	12 (28.6%)	
Presence	32 (28.3%)	13 (18.3%)	19 (45.2%)	
Unknown	43 (38.1%)	32 (45.1%)	11 (26.2%)	
Lymphovascular invasion, n (%)				0.001
Absence	42 (37.2%)	29 (40.8%)	13 (31.0%)	
Presence	21 (18.6%)	6 (8.5%)	15 (35.7%)	
Unknown	50 (44.2%)	36 (50.7%)	14 (33.3%)	
Number of lymph nodes removed at surgery	13 [10; 17]	13 [9; 17]	13 [11; 17]	0.510

CEA, carcinoembryonic antigen; CA19-9, carbohydrate antigen 199; APE, abdominoperineal excision; LAR, low anterior resection

## Analyses of configuration criterion

This study summarized the morphological characteristics of these lymph nodes (Table 2, Figure S3). Significant differences were observed between the pN+ and pN- groups across the three modalities except for the shape category of CE-CT and T1CE ( $P=0.550$ ). More than half of the pN- patients had spherical shapes (76.1% for CE-CT, 66.2% for T2WI, 70.4% for T1CE). Most pN+ patients had any texture change (71.4% for CE-CT, 71.4% for T2WI, and 73.8% for T1CE).

## Node-RADS performance analysis

In each of the 113 patients, the LN with the highest Node-RADS score was evaluated for each modality. Among 19

(16.8%) patients, the LN with the highest score differed across the three modalities. The results illustrate the distribution of Node-RADS scores of patients with pN+ and pN- groups (Fig. 2, Table S3). Compared with the pN- group, the Node-RADS scores were higher in the pN+ group ( $P<0.001$ ). The diagnostic performance metrics of Node-RADS and SAD measurements across all imaging modalities are summarized in Table 3, and detailed statistical parameters are presented in Table S4. The ROC curves demonstrate the comparative performance of Node-RADS and SAD measurements on CE-CT, T2WI, and T1CE (Fig. 3A-C), as well as the diagnostic capabilities of Node-RADS across the three modalities (Fig. 3D).

## Diagnostic performance on CE-CT

The Node-RADS evaluation on CE-CT demonstrated an AUC of 0.838, with a sensitivity of 78.57%, specificity of 91.55%, and accuracy of 86.73%. The diagnostic performance was significantly superior to SAD measurements (AUC: 0.838 vs. 0.744,  $P=0.011$ ), with an IDI improvement of 18.8% ( $P=0.038$ ).

## Diagnostic performance on MRI

On T2WI, Node-RADS achieved an AUC of 0.845, sensitivity of 78.57%, specificity of 92.96%, and accuracy of 87.61%. The performance significantly exceeded that of SAD measurements (AUC: 0.845 vs. 0.747,  $P=0.009$ ), with an IDI improvement of 23.1% ( $P=0.008$ ).

Similarly, on T1CE sequences, Node-RADS showed an AUC of 0.853, sensitivity of 76.19%, specificity of 91.55%, and accuracy of 85.84%, thus outperforming SAD measurements (AUC: 0.853 vs. 0.786,  $P=0.008$ ), with an IDI improvement of 22.8% ( $P=0.006$ ).

## Comparison between imaging modalities

No statistically significant differences were observed in diagnostic performance among the three modalities (CE-CT vs. T2WI:  $P=0.858$ ; CE-CT vs. T1CE:  $P=0.624$ ; T2WI vs. T1CE:  $P=0.673$ ). McNemar tests showed comparable sensitivity, specificity, and accuracy between paired modalities after Bonferroni correction (all  $P=1.000$ ).

When combining multiple modalities, the Node-RADS<sub>max</sub> approach (using the highest score across modalities) yielded an AUC of 0.866 (95% CI: 0.787–0.945), with a sensitivity of 83.33%, specificity of 88.73%, and accuracy of 86.73%. The Node-RADS<sub>min</sub> approach (using the lowest score) showed an AUC of 0.830 (95% CI: 0.743–0.918), with sensitivity of 69.05%, specificity of 95.77%, and accuracy of 85.84%. The improvements of Node-RADS<sub>max</sub> compared

**Table 2** Comparison of characteristics between pN- and pN+ patients in CE-CT, T2WI and T1CE

Characteristics	CE-CT			T2WI			T1CE		
	pN-	pN+	<i>p</i>	pN-	pN+	<i>p</i>	pN-	pN+	<i>p</i>
<b>Size</b>			0.001			0.001			<0.001
Normal	27 (38.0%)	4 (9.5%)		33 (46.5%)	6 (14.3%)		38 (53.5%)	5 (11.9%)	
Enlarged	44 (62.0%)	38 (90.5%)		38 (53.5%)	36 (85.7%)		33 (46.5%)	37 (88.1%)	
Bulk	0	0		0	0		0	0	
<b>Configuration</b>									
<b>Texture</b>			<0.001			<0.001			<0.001
Homogeneous	67 (94.4%)	12 (28.6%)		64 (90.1%)	12 (28.6%)		63 (88.7%)	11 (26.2%)	
Heterogeneous	3 (4.2%)	22 (52.4%)		6 (8.5%)	21 (50.0%)		2 (2.8%)	7 (16.7%)	
Focal necrosis	1 (1.4%)	7 (16.7%)		1 (1.4%)	4 (9.5%)		4 (5.6%)	12 (28.6%)	
Gross necrosis	0 (0.0%)	1 (2.4%)		0 (0.0%)	5 (11.9%)		2 (2.8%)	12 (28.6%)	
<b>Border</b>			<0.001			<0.001			<0.001
Smooth	68 (95.8%)	26 (61.9%)		64 (90.1%)	20 (47.6%)		65 (91.5%)	14 (33.3%)	
Irregular	3 (4.2%)	16 (38.1%)		7 (9.9%)	22 (52.4%)		6 (8.5%)	28 (66.7%)	
<b>Shape</b>			0.55			0.048			0.07
Oval <sup>a</sup>	17 (23.9%)	8 (19.0%)		24 (33.8%)	7 (16.7%)		21 (29.6%)	6 (14.3%)	
Spherical <sup>b</sup>	54 (76.1%)	34 (81.0%)		47 (66.2%)	35 (83.3%)		50 (70.4%)	36 (85.7%)	

<sup>a</sup>Any shape with preserved fatty hilum or kidney-bean-like or oval without fatty hilum. <sup>b</sup>Spherical without fatty hilum.

to individual modalities (CE-CT: 11.1%,  $P=0.149$ ; T2WI: 7.1%,  $P=0.320$ ; T1CE: 3.6%,  $P=0.590$ ) were not statistically significant.

### Node-RADS 3 classification analysis

To discuss how to report Node-RADS 3 further, we dichotomized the Node-RADS scores based on the different cut-off values, classifying them as LN clinical N- and clinical N+ groups. The results show the diagnostic performance between the two groups across the three modalities (Table S5). The diagnostic performance exhibited a substantial enhancement when Node-RADS 3 was grouped as clinical N- across three modalities. For CE-CT, the AUC demonstrated a notable improvement from 0.654 to 0.851 ( $P<0.0001$ ), with sensitivity maintaining comparability ( $P=0.250$ ) while specificity exhibited a substantial enhancement ( $P<0.001$ ). For T2WI, the AUC increased from 0.703 to 0.858 ( $P<0.0001$ ), with no statistically significant change in sensitivity ( $P=0.250$ ) but a marked improvement in specificity ( $P<0.001$ ). For T1CE, the AUC increased from 0.731 to 0.839 ( $P=0.0028$ ), and there was no statistically significant difference in sensitivity ( $P=0.125$ ). However, a significant increase was observed in specificity ( $P<0.001$ ). When Node-RADS 3 was classified into the clinical N-group, the diagnostic accuracy of all three modalities exhibited a significant improvement. For CE-CT, the accuracy increased from 60.18 to 86.73% ( $P<0.001$ ); for T2WI, it increased from 66.37 to 87.61% ( $P<0.001$ ); and for T1CE, it increased from 69.91 to 85.84% ( $P=0.001$ ).

### Discussion

The present study investigated the value of the Node-RADS v1.0 in assessing LN status on CE-CT, T2WI, and T1CE images in rectal cancer patients. The results indicated that the efficacy of Node-RADS surpassed that of SAD alone ( $P=0.008$ – $0.011$ ). Furthermore, no statistically significant differences were observed between the diagnostic performances of CE-CT, T2WI, and T1CE in Node-RADS assessment ( $P=0.624$ – $0.858$ ), suggesting that Node-RADS v1.0 displays consistent and comparable diagnostic efficacy across diverse imaging modalities. Additionally, we defined Node-RADS<sub>max</sub> as the maximum Node-RADS score among CE-CT, T2WI, and T1CE images for each patient. Although Node-RADS<sub>max</sub> demonstrated an elevated AUC of 0.863 (sensitivity 80.95%, specificity 92.96%, accuracy 88.50%) compared to any solitary modality, the enhancement was not statistically significant ( $P=0.149$ – $0.590$ ). These findings suggest that Node-RADS applied to CE-CT, T2WI, and T1CE exhibits significant potential and demonstrates promising diagnostic performance in patients with rectal cancer.

An accurate primary lymph node assessment is imperative in informing both treatment planning and prognostic evaluation, including decisions regarding neoadjuvant therapy and the necessity of lateral pelvic lymph node dissection (Beets-Tan 2013; MERCURY Study Group 2006; Horvat et al. 2019). According to the consensus of prominent radiological societies, including ESGAR and SAR Colorectal and Anal Cancer Disease-Focused Panel, lymph node evaluation encompasses both morphological features, such as border irregularity, signal heterogeneity, and spherical configuration, and dimensional measurements along the short axis

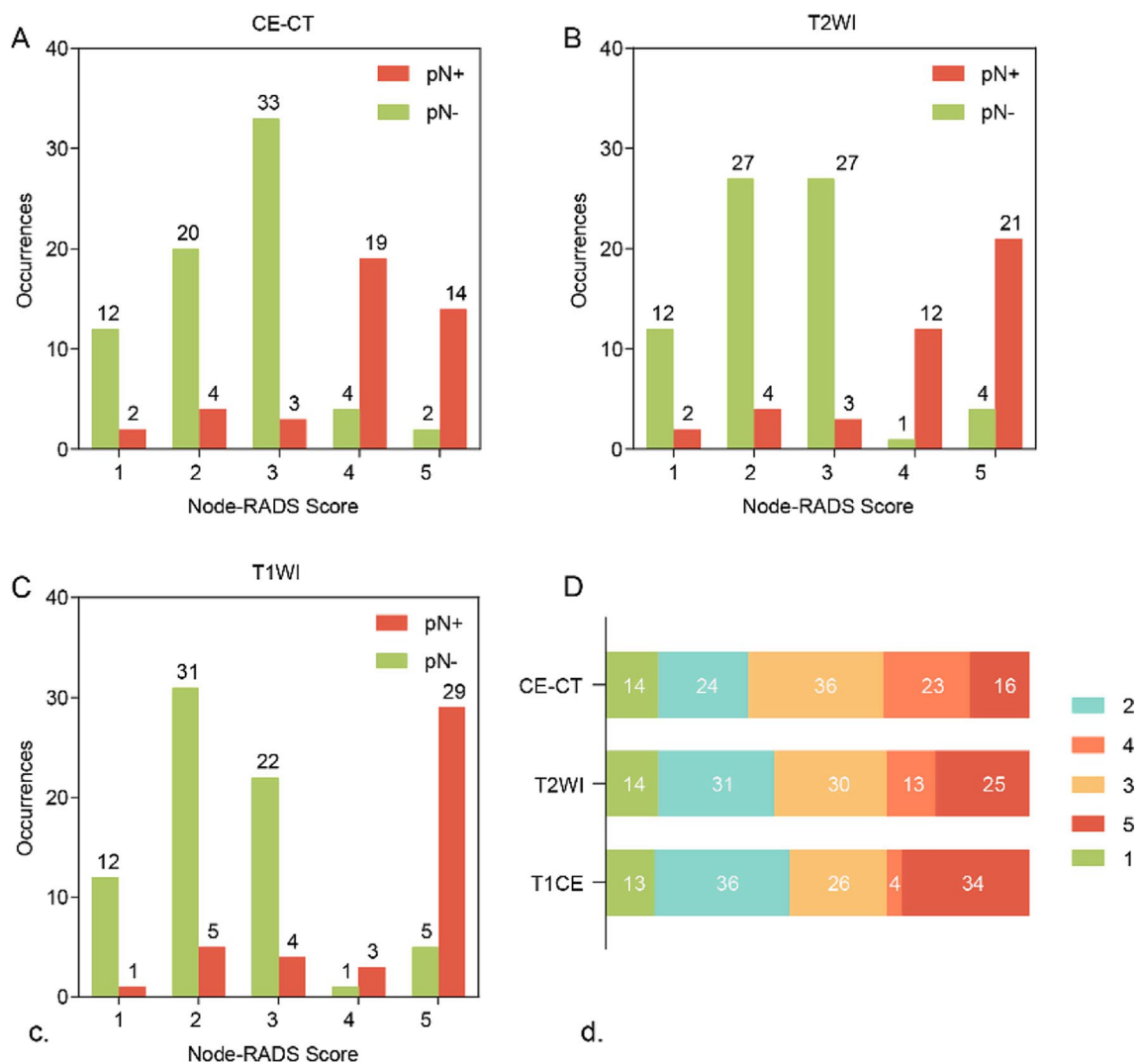


**Fig. 2** The distribution of Node-RADS score on CE-CT, T2WI and T1CE. (A–C) Comparisons of Node-RADS score occurrences based on the histopathological lymph node status (pN-, green bars, pN+, orange bars). (D) An overall distribution of Node-RADS scores across three modalities

**Table 3** Diagnostic performance of MRI and CT for the prediction of lymph node status

	Modalities	Cut-off value	Sensitivity (%)	Specificity (%)	Youden Index	ACC(%)	AUC(95% CI)
Node-RADS	CE-CT	3.5	78.57	91.55	0.701	86.73	0.838 (0.750-0.926)
	T2WI	3.5	78.57	92.96	0.715	87.61	0.845 (0.759-0.930)
	T1CE	3.5	76.19	91.55	0.677	85.84	0.853 (0.773-0.932)
	Node-RADS <sub>max</sub>	3.5	83.33	88.73	0.721	86.73	0.866 (0.787-0.945)
	Node-RADS <sub>min</sub>	3.5	69.05	95.77	0.648	85.84	0.830 (0.743-0.918)
SAD	CE-CT	7.35	52.38	85.92	0.383	73.45	0.744 (0.649-0.839)
	T2WI	6.10	71.43	71.83	0.433	71.68	0.747 (0.652-0.842)
	T1CE	5.95	73.81	74.65	0.485	74.34	0.786 (0.698-0.874)

ACC, accuracy; AUC, area under the receiver operating characteristic curve; 95% CI, 95% confidence interval

(Kusters et al. 2010). A recent survey conducted in the UK (Robinson et al. 2024) revealed that most radiologists preferred comprehensive assessment approaches. Among these, 18 out of 75 (24%) respondents utilized a combination of ESGAR, while 16 out of 75 (21.3%) employed a combination of ESGAR criteria with chemical shift. In contrast, only

1 out of 75 (1.3%) respondents relied solely on lymph node size for assessment. This survey underscores the absence of standardization in lymph node assessment among radiologists. While ESGAR criteria are commonly employed, their application is inherently constrained, as they were developed explicitly for MRI evaluation of rectal cancer only



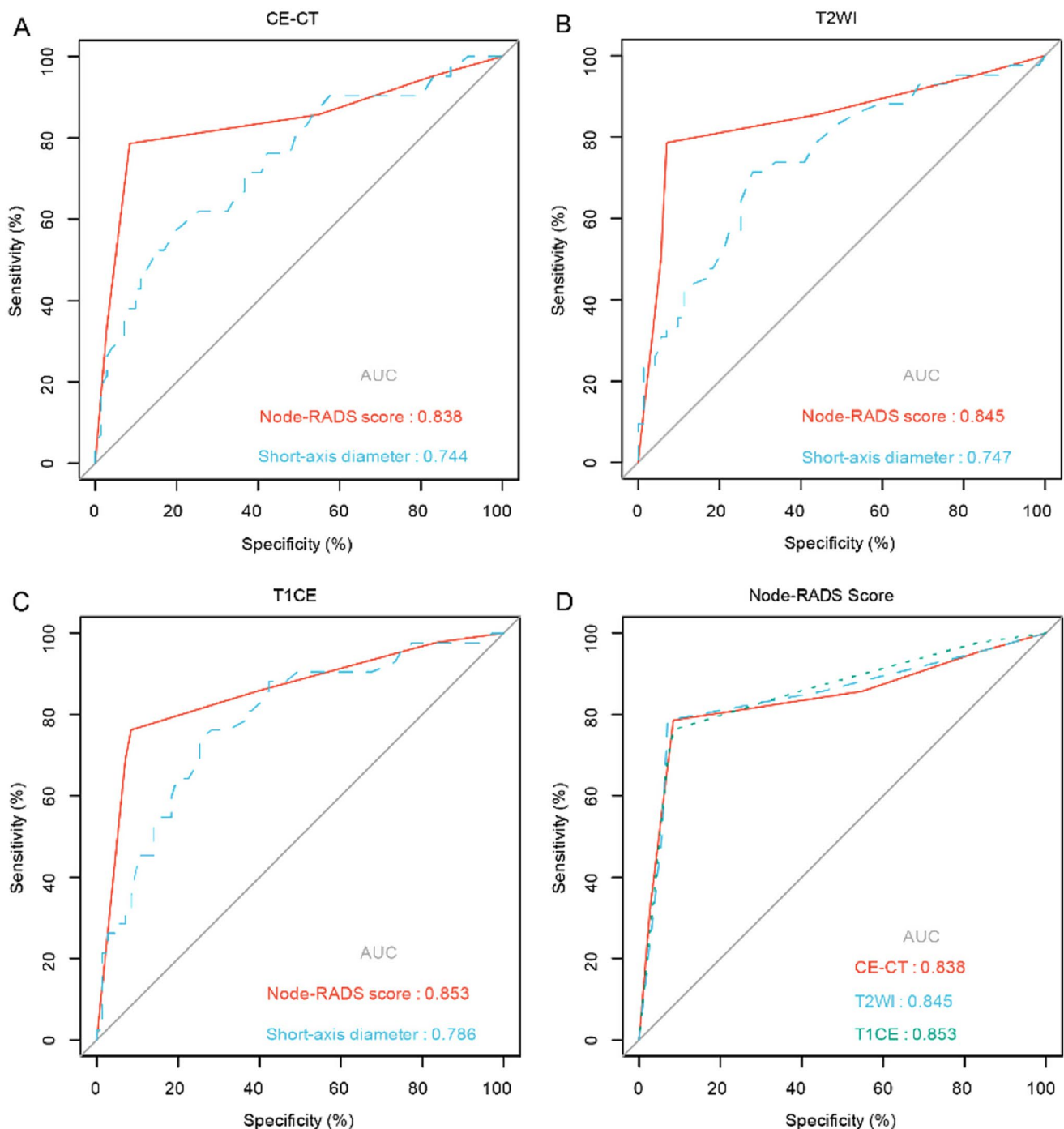


**Fig. 3** Receiver operating characteristic (ROC) curve of Node-RADS score and short-axis diameter (SAD). (A–C) The ROC curve of Node-RADS and the corresponding SAD used to discriminate lymph node

status on (A) CE-CT, (B) T2WI, and (C) T1CE. (D) ROC curve of the Node-RADS score as a predictor of pathological metastasis for regional lymph nodes of rectal cancer on CE-CT, T2WI, and T1CE

(Beets-Tan et al. 2018). The advent of Node-RADS signifies a substantial progression in standardized and reproducible lymph node evaluation. A notable finding emerged from the research conducted by Niu et al., which demonstrated that Node-RADS exhibited superior diagnostic efficacy compared to the ESGAR criteria (Niu et al. 2025). In their study

of rectal cancer, the diagnostic performance of Node-RADS showed sensitivity ranging from 73.20–84.85%, specificity from 60.90–84.09%, accuracy from 70.50–83.76%, and AUC from 0.758 to 0.862 across different imaging modalities (Niu et al. 2024, 2025). Notably, Niu et al. demonstrated that Node-RADS outperformed SAD in diagnostic

performance (all  $P < 0.05$ ). Similarly, in our study, Node-RADS also showed superior diagnostic accuracy compared to SAD alone in treatment-naïve patients. Specifically, our study demonstrated high diagnostic performance, with sensitivity ranging from 76.19–78.57%, specificity from 91.55–92.96%, and accuracy from 85.84–87.61%. Furthermore, there was a substantial improvement in IDI (18.8%–23.1%) compared to SAD alone in treatment-naïve patients. The present study demonstrated a comprehensive improvement in diagnostic accuracy across all imaging modalities. Interestingly, this study revealed comparable diagnostic performance of Node-RADS across CE-CT, T2WI, and T1CE modalities, with no significant differences in AUCs, sensitivity, specificity, and accuracy among the three modalities. The consistent diagnostic performance among different imaging modalities suggests that Node-RADS maintains reliable performance regardless of the imaging technique used. However, future prospective studies are needed to validate these findings in post-neoadjuvant therapy settings, as our current study focused solely on primary staging in treatment-naïve patients.

According to the Node-RADS, the classification of Node-RADS 3 should be guided by the stage and histologic grade of the primary tumor (Elsholtz et al. 2021). Our findings suggest that classifying Node-RADS 3 as clinical N- significantly improves diagnostic performance across all three imaging modalities, particularly in terms of specificity and diagnostic accuracy, while sensitivity remains comparable. Consequently, classifying Node-RADS 3 as clinical N-negative may help mitigate the occurrence of false-positive findings when compared with the classification of positive, which could lead to a reduction in overtreatment in clinical practice.

The optimal imaging approach for lymph node evaluation remains a subject of debate, particularly regarding the selection of different MRI sequences (Bipat et al. 2004; Peeters et al. 2005). While the NCCN guidelines state that T1CE is not mandatory for primary staging in rectal cancer (Benson et al. 2022), the optimal protocol remains debatable. The Node-RADS framework reflects this perspective, mandating contrast enhancement for CT due to its lower resolution while making it optional for MRI given its inherently high soft tissue contrast. Studies have shown that gadolinium-based contrast agents may improve MRI sensitivity and specificity for LN evaluation by identifying nodal necrosis, an indicator of metastasis (Clament and Luciani 2004; Misselwitz et al. 2004). A recent systematic consensus study employed the RAND-UCLA Appropriateness Method to evaluate rectal MRI protocols (Nougaret et al. 2022). Despite two rounds of expert panel discussions, no consensus ( $\geq 80\%$  agreement) was reached regarding the necessity of gadolinium-based contrast administration. Our

protocol selected delayed-phase T1CE images (approximately 5 min post-contrast) using the volumetric interpolated breath-hold examination (VIBE) sequence, which offers high spatial resolution and excellent fat suppression. The Node-RADS guidelines specify the appropriate parenchymal phase for CT acquisition but do not mandate contrast-enhanced MRI or define specific post-contrast phases. In this study, we adopted the delayed phase for contrast-enhanced T1-weighted imaging based on CT phase selection, and this phase can better demonstrate internal nodal architecture. Further research is required to refine and standardize the optimal post-contrast timing for MRI. However, no significant enhancement in diagnostic performance was observed between T1CE and T2WI (AUC: 0.853 vs. 0.845,  $P > 0.05$ ). These findings suggest that routine administration of contrast medium may not provide substantial additional benefit for nodal staging, which is consistent with current NCCN guidelines. Notably, while its role in nodal staging remains controversial, some studies suggest that contrast enhancement may be beneficial in specific clinical scenarios, such as improving T3 cancer detection and measuring the distance to the anal sphincter (Alberda et al. 2013; Corines et al. 2018). Further research is needed to investigate the relationship between Node-RADS categorization and the diagnostic value of contrast-enhanced imaging in different clinical scenarios and patient subgroups.

Standardized reporting systems have demonstrated the potential to enhance the quality of radiological assessments (Nörenberg et al. 2017). Previous research indicated that traditional free-text reports often lack essential diagnostic information, with one investigation noting that over half of the oncologic staging reports missed crucial elements for treatment planning (Patel et al. 2018). Although the soft tissue resolution of CT is inherently lower than that of MRI for local staging, structured reporting templates might help optimize the diagnostic performance of CT in rectal cancer evaluation. In the present study, CE-CT exhibited comparable diagnostic performance to MRI sequences (T2WI and T1CE) in LNI assessment, with the added benefit of facilitating distant metastasis evaluation. While combining multiple modalities enhanced diagnostic efficacy, this discrepancy did not attain statistical significance. Subsequent studies are necessary to assess the impact of the Node-RADS (Node Reporting and Data System) standardized reporting system on CT diagnostic performance in rectal cancer staging. This investigation would be particularly valuable since Node-RADS provides a standardized reporting framework that might optimize CT staging for patients with contraindications to MRI, potentially offering a structured approach to maintain diagnostic quality when MRI is not feasible.

Despite its advantages, the Node-RADS has several limitations that warrant further refinement. For example, there

is a need for standardized technical parameters for CT and MRI, the development of clinically applicable structured reporting templates, and the incorporation of additional imaging features such as functional imaging parameters. Furthermore, the current Node-RADS definition of bulk nodes (any axis  $\geq 30$  mm) may need modification, as such criteria are rarely encountered in rectal cancer. In the present cohort of 113 patients, none of the lymph nodes met the criteria for bulk classification. Further studies are necessary to explore and refine these aspects in future iterations of Node-RADS, intending to optimize its clinical application.

The challenges associated with lymph node staging extend beyond the Node-RADS system itself. The diagnostic performance of lymph node staging remains inferior to that of T staging due to fundamental imaging limitations (Li et al. 2014). The primary obstacle lies in the inability of conventional imaging to detect metastasis in small lymph nodes, while larger nodes often present confounding factors such as fat infiltration and calcification (Kucharczyk and Henkelman 1994; Wang et al. 2005). While advanced imaging techniques, such as MRI contrast agents (ultra-small superparamagnetic iron oxide [USPIO] and gadofosveset), have demonstrated potential in enhancing nodal characterization, their clinical implementation remains constrained due to availability and safety concerns (Koh et al. 2010; McDonald and McDonald 2020). Acknowledging these imaging limitations is paramount as Node-RADS continues to evolve and adapt to clinical requirements.

Despite the encouraging results, our study is not without its limitations. Firstly, the retrospective design of this study has inherent limitations, including the absence of node-by-node radiologic-pathologic correlation in the analysis. Secondly, the study cohort was constrained to patients who underwent both preoperative CT and MRI, potentially introducing selection bias and limiting its representation of the broader patient population. Thirdly, the inclusion criteria were restricted to patients who underwent upfront surgery without preoperative therapy, aiming to ascertain the performance of Node-RADS in primary staging. Further research is needed to evaluate its diagnostic value in post-neoadjuvant therapy assessment. The sample size was relatively small; however, cases were selected based on strict criteria. Finally, Node-RADS performance may vary depending on the radiologist's experience. Further research and multi-center studies are needed to validate Node-RADS v1.0 in rectal cancer. As understanding of Node-RADS evolves, future versions may improve diagnostic performance.

In conclusion, Node-RADS demonstrated superior diagnostic performance over SAD measurements across all three imaging modalities. Furthermore, Node-RADS exhibited comparable diagnostic efficacy among CE-CT, T2WI, and T1CE in assessing lymph node involvement for primary

rectal cancer staging. These findings highlight the potential of Node-RADS v. 1.0 as a standardized and reliable system for lymph node evaluation, validating its cross-modality applicability in the primary staging of rectal cancer.

**Supplementary Information** The online version contains supplementary material available at <https://doi.org/10.1007/s00432-025-06196-9>.

**Author contributions** Li Jiang: data collection, project development, manuscript writing, data analysis; Zijian Zhuang: data collection, project development; Xi Tang: data analysis; Fugang Zhang: data collection; Haitao Zhu: manuscript writing, data analysis; Xuewen Xu: data collection; Dongqing Wang: project development, manuscript writing; Lirong Zhang: project development, Manuscript Editing. All authors reviewed the manuscript.

**Funding** This work was supported by the National Natural Science Foundation of China (grant number 82272066), the Key Project of Jiangsu Provincial Health Commission (grant number K2019024), the Natural Science Foundation of Jiangsu Province (grant number BK20191223), and the Scientific Research project of the Jinshan Talent Training Program for high-level leading Talents (grant number YLJ202111).

**Data availability** The datasets generated during and/or analysed during the current study are available from the corresponding author on reasonable request.

## Declarations

**Ethical approval** All patients provided informed consent and agreed to participate in the study. The present study was approved by the ethical review board of the Affiliated Hospital of Jiangsu University (reference number SWYXLL20190225-3).

**Competing interests** The authors declare no competing interests.

**Open Access** This article is licensed under a Creative Commons Attribution-NonCommercial-NoDerivatives 4.0 International License, which permits any non-commercial use, sharing, distribution and reproduction in any medium or format, as long as you give appropriate credit to the original author(s) and the source, provide a link to the Creative Commons licence, and indicate if you modified the licensed material. You do not have permission under this licence to share adapted material derived from this article or parts of it. The images or other third party material in this article are included in the article's Creative Commons licence, unless indicated otherwise in a credit line to the material. If material is not included in the article's Creative Commons licence and your intended use is not permitted by statutory regulation or exceeds the permitted use, you will need to obtain permission directly from the copyright holder. To view a copy of this licence, visit <http://creativecommons.org/licenses/by-nc-nd/4.0/>.

## References

- Akkaya H, Dilek O, Özdemir S et al (2024) Rectal cancer and lateral lymph node staging: interobserver agreement and success in predicting locoregional recurrence. *Diagnostics (Basel)* 14. <https://doi.org/10.3390/diagnostics14222570>

- Alberda WJ, Dassen HP, Dwarkasing RS et al (2013) Prediction of tumor stage and lymph node involvement with dynamic contrast-enhanced MRI after chemoradiotherapy for locally advanced rectal cancer. *Int J Colorectal Dis* 28:573–580. <https://doi.org/10.1007/s00384-012-1576-6>
- Beets-Tan RG (2013) Pretreatment MRI of lymph nodes in rectal cancer: an opinion-based review. *Colorectal Dis* 15:781–784. <https://doi.org/10.1111/codi.12300>
- Beets-Tan RGH, Lambregts DMJ, Maas M et al (2018) Magnetic resonance imaging for clinical management of rectal cancer: updated recommendations from the 2016 European society of Gastrointestinal and abdominal radiology (ESGAR) consensus meeting. *Eur Radiol* 28:1465–1475. <https://doi.org/10.1007/s00330-017-5026-2>
- Benson AB, Venook AP, Al-Hawary MM et al (2022) Rectal cancer, version 2.2022, NCCN clinical practice guidelines in oncology. *J Natl Compr Canc Netw* 20:1139–1167. <https://doi.org/10.6004/jnccn.2022.0051>
- Bipat S, Glas AS, Slors FJ et al (2004) Rectal cancer: local staging and assessment of lymph node involvement with endoluminal US, CT, and MR imaging—a meta-analysis. *Radiology* 232:773–783. <https://doi.org/10.1148/radiol.2323031368>
- Bray F, Laversanne M, Sung H et al (2024) Global cancer statistics 2022: GLOBOCAN estimates of incidence and mortality worldwide for 36 cancers in 185 countries. *CA Cancer J Clin* 74:229–263. <https://doi.org/10.3322/caac.21834>
- Clément O, Luciani A (2004) Imaging the lymphatic system: possibilities and clinical applications. *Eur Radiol* 14:1498–1507. <https://doi.org/10.1007/s00330-004-2265-9>
- Corines MJ, Nougaret S, Weiser MR et al (2018) Gadolinium-Based contrast agent during pelvic MRI: contribution to patient management in rectal cancer. *Dis Colon Rectum* 61:193–201. <https://doi.org/10.1097/dcr.0000000000000925>
- Dekker E, Tanis PJ, Vleugels JLA et al (2019) Colorectal cancer. *Lancet* 394:1467–1480. [https://doi.org/10.1016/s0140-6736\(19\)32319-0](https://doi.org/10.1016/s0140-6736(19)32319-0)
- Elsholtz FHJ, Asbach P, Haas M et al (2021) Introducing the node reporting and data system 1.0 (Node-RADS): a concept for standardized assessment of lymph nodes in cancer. *Eur Radiol* 31:6116–6124. <https://doi.org/10.1007/s00330-020-07572-4>
- Fernandes MC, Gollub MJ, Brown G (2022) The importance of MRI for rectal cancer evaluation. *Surg Oncol* 43:101739. <https://doi.org/10.1016/j.suronc.2022.101739>
- Horvat N, Carlos Tavares Rocha C, Clemente Oliveira B et al (2019) MRI of rectal cancer: tumor staging, imaging techniques, and management. *Radiographics* 39:367–387. <https://doi.org/10.1148/rg.2019180114>
- Kapiteijn E, Marijnen CA, Nagtegaal ID et al (2001) Preoperative radiotherapy combined with total mesorectal excision for resectable rectal cancer. *N Engl J Med* 345:638–646. <https://doi.org/10.1056/NEJMoa010580>
- Koh DM, George C, Temple L et al (2010) Diagnostic accuracy of nodal enhancement pattern of rectal cancer at MRI enhanced with ultrasmall superparamagnetic iron oxide: findings in pathologically matched mesorectal lymph nodes. *AJR Am J Roentgenol* 194:W505–513. <https://doi.org/10.2214/ajr.08.1819>
- Kucharczyk W, Henkelman RM (1994) Visibility of calcium on MR and CT: can MR show calcium that CT cannot? *AJNR Am J Neuroradiol* 15:1145–1148
- Kusters M, Marijnen CA, van de Velde CJ et al (2010) Patterns of local recurrence in rectal cancer; a study of the Dutch TME trial. *Eur J Surg Oncol* 36:470–476. <https://doi.org/10.1016/j.ejso.2009.11.011>
- Li J, Guo BC, Sun LR et al (2014) TNM staging of colorectal cancer should be reconsidered by T stage weighting. *World J Gastroenterol* 20:5104–5112. <https://doi.org/10.3748/wjg.v20.i17.5104>
- Loch FN, Beyer K, Kreis ME et al (2024) Diagnostic performance of node reporting and data system (Node-RADS) for regional lymph node staging of gastric cancer by CT. *Eur Radiol* 34:3183–3193. <https://doi.org/10.1007/s00330-023-10352-5>
- McDonald JS, McDonald RJ (2020) MR imaging safety considerations of gadolinium-Based contrast agents: gadolinium retention and nephrogenic systemic fibrosis. *Magn Reson Imaging Clin N Am* 28:497–507. <https://doi.org/10.1016/j.mric.2020.06.001>
- MERCURY Study Group (2006) Diagnostic accuracy of preoperative magnetic resonance imaging in predicting curative resection of rectal cancer: prospective observational study. *BMJ* 333:779. <https://doi.org/10.1136/bmj.38937.646400.55>
- Meyer HJ, Schnarkowski B, Pappisch J et al (2022) CT texture analysis and node-RADS CT score of mediastinal lymph nodes - diagnostic performance in lung cancer patients. *Cancer Imaging* 22:75. <https://doi.org/10.1186/s40644-022-00506-x>
- Misselwitz B, Platzek J, Weinmann HJ (2004) Early MR lymphography with gadofluorine M in rabbits. *Radiology* 231:682–688. <https://doi.org/10.1148/radiol.2313021000>
- Niu Y, Wen L, Yang Y et al (2024) Diagnostic performance of node reporting and data system (Node-RADS) for assessing mesorectal lymph node in rectal cancer by CT. *BMC Cancer* 24:716. <https://doi.org/10.1186/s12885-024-12487-0>
- Niu Y, Yu S, Chen P et al (2025) Diagnostic performance of Node-RADS score for mesorectal lymph node metastasis in rectal cancer. *Abdom Radiol (NY)* 50:38–48. <https://doi.org/10.1007/s00261-024-04497-0>
- Nörenberg D, Sommer WH, Thasler W et al (2017) Structured reporting of rectal magnetic resonance imaging in suspected primary rectal cancer: potential benefits for surgical planning and interdisciplinary communication. *Invest Radiol* 52:232–239. <https://doi.org/10.1097/rli.0000000000000336>
- Nougaret S, Rousset P, Gormly K et al (2022) Structured and shared MRI staging lexicon and report of rectal cancer: A consensus proposal by the French radiology group (GRERCAR) and surgical group (GRECCAR) for rectal cancer. *Diagn Interv Imaging* 103:127–141. <https://doi.org/10.1016/j.diii.2021.08.003>
- Patel A, Rockall A, Guthrie A et al (2018) Can the completeness of radiological cancer staging reports be improved using proforma reporting? A prospective multicentre non-blinded interventional study across 21 centres in the UK. *BMJ Open* 8:e018499. <https://doi.org/10.1136/bmjopen-2017-018499>
- Pediconi F, Maroncelli R, Pasculli M et al (2024) Performance of MRI for standardized lymph nodes assessment in breast cancer: are we ready for Node-RADS? *Eur Radiol* 34:7734–7745. <https://doi.org/10.1007/s00330-024-10828-y>
- Peeters KC, van de Velde CJ, Leer JW et al (2005) Late side effects of short-course preoperative radiotherapy combined with total mesorectal excision for rectal cancer: increased bowel dysfunction in irradiated patients—a Dutch colorectal cancer group study. *J Clin Oncol* 23:6199–6206. <https://doi.org/10.1200/jco.2005.14.779>
- Robinson E, Balasubramaniam R, Hameed M et al (2024) Survey of rectal cancer MRI technique and reporting tumour descriptors in the UK: a multi-centre British society of Gastrointestinal and abdominal radiology (BSGAR) audit. *Clin Radiol* 79:117–123. <https://doi.org/10.1016/j.crad.2023.10.025>
- Siegel RL, Wagle NS, Cercek A et al (2023) Colorectal cancer statistics, 2023. *CA Cancer J Clin* 73:233–254. <https://doi.org/10.3322/caac.21772>
- Tessler FN, Middleton WD, Grant EG, et al. (2017) ACR Thyroid Imaging, Reporting and Data System (TI-RADS): white paper of the ACR TI-RADS committee. *J Am Coll Radiol* 14:587–595. <https://doi.org/10.1016/j.jacr.2017.01.046>
- Turkbey B, Rosenkrantz AB, Haider MA, et al. (2019) Prostate imaging reporting and data system version 2.1: 2019 Update of



- prostate imaging reporting and data system version 2. *Eur Urol* 76:340–351. <https://doi.org/10.1016/j.eururo.2019.02.033>
- Wang C, Zhou ZG, Wang Z et al (2005) Nodal spread and micrometastasis within mesorectum. *World J Gastroenterol* 11:3586–3590. <https://doi.org/10.3748/wjg.v11.i23.3586>
- Weiser MR (2018) AJCC 8th edition: colorectal cancer. *Ann Surg Oncol* 25:1454–1455. <https://doi.org/10.1245/s10434-018-6462-1>
- Wu Q, Lou J, Liu J et al (2024) Performance of node reporting and data system (node-RADS): a preliminary study in cervical cancer. *BMC Med Imaging* 24:28. <https://doi.org/10.1186/s12880-024-01205-8>
- Zhong J, Mao S, Chen H et al (2024) Node-RADS: a systematic review and meta-analysis of diagnostic performance, category-wise malignancy rates, and inter-observer reliability. *Eur Radiol*. <https://doi.org/10.1007/s00330-024-11160-1>

**Publisher's note** Springer Nature remains neutral with regard to jurisdictional claims in published maps and institutional affiliations.